

# Co(II), Ni(II), Cu(II) and Zn(II) complexes of tetraphenylazadipyrromethene†

Aniello Palma,<sup>a</sup> John F. Gallagher,<sup>b</sup> Helge Müller-Bunz,<sup>a</sup> Joanna Wolowska,<sup>c</sup> Eric J.L. McInnes<sup>c</sup> and Donal F. O'Shea<sup>\*a</sup>

Received 10th July 2008, Accepted 12th September 2008

First published as an Advance Article on the web 5th November 2008

DOI: 10.1039/b811764k

The synthesis, crystallographic and spectroscopic properties of four divalent isomorphous metal complexes of tetraphenylazadipyrromethene are described.

## Introduction

The development of new chromophores with spectral properties in the near-infrared (NIR) and visible red spectral regions is an area of expanding research interest. The synthesis and photophysical characteristics of the BF<sub>2</sub> chelated tetraarylazadipyrromethanes **1** (Fig. 1) have been recently reported from our laboratory as having high extinction coefficients and substituent variable fluorescence quantum yields in the 650–750 nm spectral region.<sup>1</sup> To date, these favourable spectroscopic parameters have indicated potential applications in photodynamic therapy,<sup>1a–d</sup> as fluorescent chemosensors<sup>1f–h,2</sup> and as *in vitro* fluorophores.<sup>1i</sup>

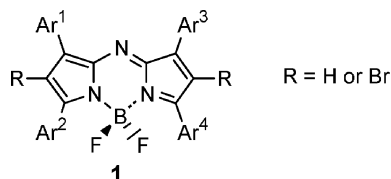


Fig. 1 BF<sub>2</sub>-chelated tetraarylazadipyrromethenes.

The penultimate step in the synthesis of these compounds is the formation of the BF<sub>2</sub> chelate, which provides sufficient structural rigidity thereby limiting radiation-less transitions and allowing the exploitation of their excited states. The compound class **2** was first reported sixty-five years ago but remained virtually unexploited until it attracted our interest (Fig. 2).<sup>3</sup> In this original article it was reported that transition metal complexes could be formed but owing to the early date of this work no analytical data was recorded. Recently, the synthesis and properties of tricoordinate Ag<sup>I</sup>, Au<sup>I</sup> and Cu<sup>I</sup> complexes of **2** (Ar = Ph) have been described.<sup>4</sup> Herein, we describe the synthesis and characteristics of three divalent transition metal derivatives Co<sup>II</sup>, Ni<sup>II</sup>, Cu<sup>II</sup> and Zn<sup>II</sup> and compare their structural and spectroscopic properties.<sup>5</sup> It is

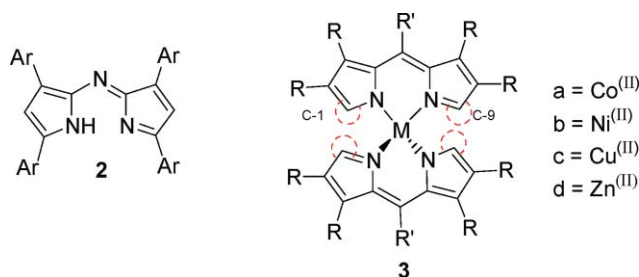


Fig. 2 Tetraarylazadipyrromethenes and dipyrryn metal complexes.

envisaged that this preliminary investigation of metal complexes may form the basis for future designed uses in catalysis, metal–organic frameworks, optical data storage and electrochromic devices to list but a few.

Related metal complexes **3** with the dipyrryn ligand have been reported for these metals in which a 1 : 2 metal–ligand complex was formed.<sup>6</sup> In several examples, it was shown that it was optimal to have the C-1 and C-9 positions unsubstituted to ensure metal complex formation as the introduction of substituents at these positions could lead to unfavourable steric interactions.<sup>6c</sup> As such, in the case of compounds **2**, it was of particular interest to assess the impact of the potential inter-ligand and metal–ligand steric interactions of the aryl rings *ortho* to the pyrrole nitrogen atoms. Possible influences would be to prevent formation of the chelate or have a pronounced effect on the stereochemistry of the ligands around the metal centre and as a consequence have an impact upon the spectroscopic properties. Herein, we have synthesised and characterised four divalent Co, Ni, Cu and Zn complexes of tetraphenylazadipyrromethene **2a** (Ar = Ph) as representative examples of this ligand class.

## Results and discussion

### Synthesis

Heating (3,5-diphenyl-1*H*-pyrrol-2-yl)-(3,5-diphenylpyrrol-2-ylidene)amine **2a** with CoCl<sub>2</sub>/NH<sub>4</sub>OAc, Ni(OAc)<sub>2</sub>, Cu(OAc)<sub>2</sub> or Zn(OAc)<sub>2</sub> for 1 h in butanol at reflux gave a clean conversion to the corresponding metal complexes **4a–d** as assessed by TLC analysis (Scheme 1).

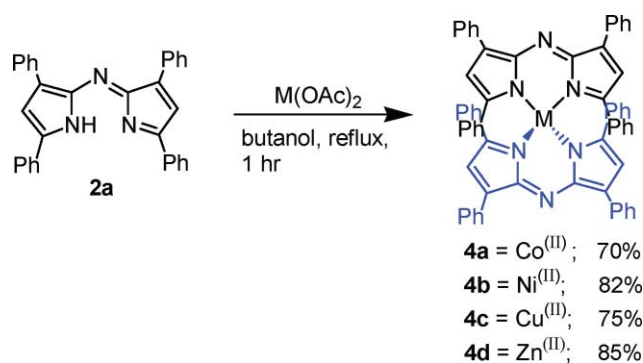
In each case, the products **4a–d** precipitated directly from the reaction mixture and were isolated as brown/black powders in high yields. Mass spectrometry confirmed a 1 : 2 stoichiometry

<sup>a</sup>Centre for Synthesis and Chemical Biology, School of Chemistry and Chemical Biology, University College Dublin, Belfield, Dublin 4, Ireland. E-mail: donal.f.oshea@ucd.ie; Tel: +353 (0)1 7162425

<sup>b</sup>School of Chemical Sciences, Dublin City University, Dublin 9, Ireland

<sup>c</sup>School of Chemistry, The University of Manchester, Oxford Road, Manchester, UK M13 9PL

† Electronic supplementary information (ESI) available: ORTEP diagrams for **4a**, **4c** and **4d**. zqTOCSY spectrum of **4b**. UV-vis spectra of **4a–d** in EtOH and toluene. EPR hyperfine coupling of **4c**. CCDC reference numbers 668337–668340. For ESI and crystallographic data in CIF or other electronic format see DOI: 10.1039/b811764k



Scheme 1

of **M-2a** ( $M = \text{Co, Ni, Cu, Zn}$ ) for each complex. Crystals, suitable for X-ray diffraction, were obtained by the slow evaporation of either chlorobenzene or DMF solutions.

### X-Ray crystallography

The structural studies of the four metal complexes **4a-d** reported herein are important in order to analyse their molecular conformations and the effects that subtle differences on metal complexation between the parent ligand and metallo-derivatives can have on a variety of physico-chemical properties. The examination of the molecular structures of the four metal complexes **4a-d** revealed that they are isomorphous in the orthorhombic system, space group *Fdd2* (no. 43) with the metal centre residing on a crystallographic two-fold axis (and with one half of the molecule residing in the asymmetric unit). The bidentate and sterically bulky ligand enforces a distorted tetrahedral geometry at the metal centre that is remarkably invariant between the four metal complexes. The metal geometry is best described as a distorted tetrahedron with angles at the metal centre  $M$  falling into the ranges from 93–95°, 102–106° and 130–138° for the various groupings of  $N-M-N$  angles (from an idealized tetrahedral 109.5°) (Table 1, Fig. 3 and ESI†).

The more ‘open’ and distorted geometry about the metal centres also facilitates two contacts (per ligand) involving the *ortho*-H atoms of the flanking phenyl groups with  $H5/H32 \cdots M$  of *ca.* 2.68 Å/2.77 Å and  $C-H \cdots M$  angles of 118°/116° (Fig. 3, bottom).

There are also subtle differences between the four metal complexes in terms of the  $M-N$  bond lengths with  $\text{Cu} < \text{Ni} < \text{Co/Zn}$ . In the Ni complex **4b**, the average  $\text{Ni}-N$  bond length of 1.97 Å is intermediate between an ideal low-spin square planar  $\text{Ni}^{\text{II}}-N$  bond length of 1.89 Å and a high spin  $\text{Ni}^{\text{II}}-N$  of 2.10 Å for 4-coordinate Ni complexes. In a related bis[*meso*-phenyl-4,6-dipyrrinato]Ni<sup>II</sup> structure **3b** ( $R' = \text{Ph}$ ,  $R = \text{H}$ ), the four  $\text{Ni}-N$

Table 1 Selected geometric data for metal complexes **4a-d**

Metal	$M-N1/N3/\text{\AA}$	$M \cdots N2/\text{\AA}$	$N1-M-N3/N3-M-N3/^\circ$ <sup>a</sup>
<b>4a</b> , Co	1.984(3)/1.974(3)	3.295(3)	94.22(11)/130.92(16)
<b>4b</b> , Ni	1.971(3)/1.965(3)	3.322(3)	92.81(14)/131.8(2)
<b>4c</b> , Cu	1.958(2)/1.949(2)	3.306(2)	93.31(8)/137.86(13)
<b>4d</b> , Zn	1.992(2)/1.983(2)	3.290(2)	94.66(8)/130.07(12)

<sup>a</sup> Symmetry operator  $1/2 - x, 1/2 - y, z$  (for convenience in Fig. 3 the symmetry equivalents are labelled with the suffix ‘a’).

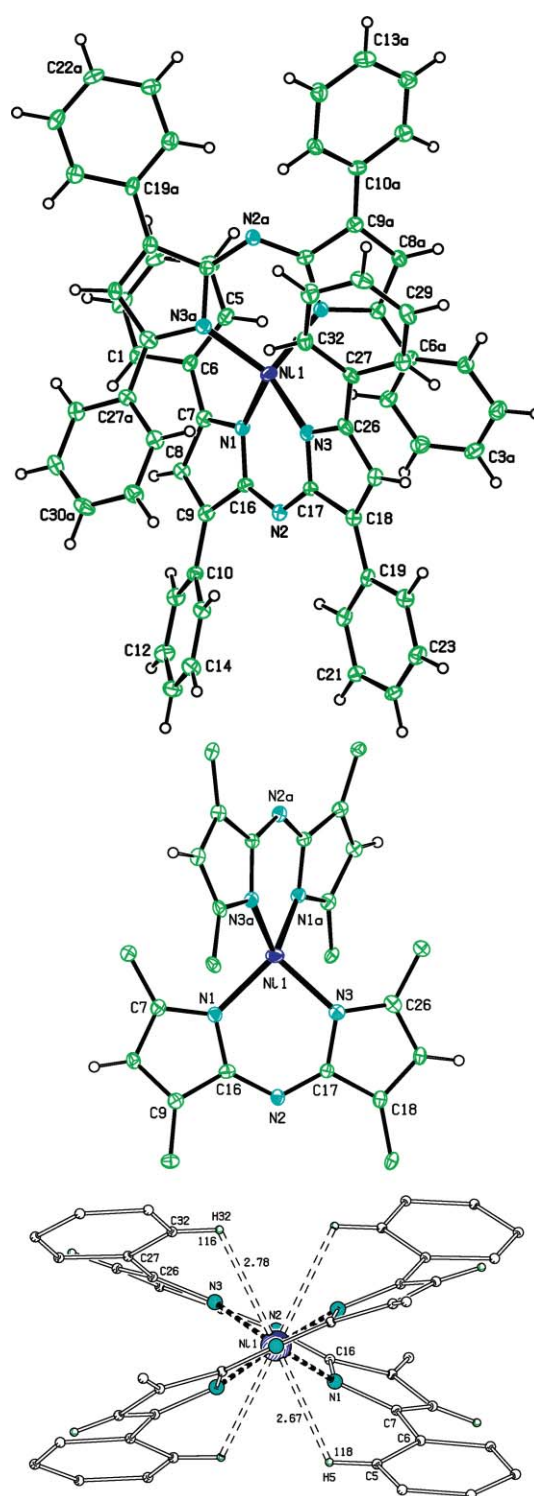


**Fig. 3** View of the Ni derivative **4b** with displacement ellipsoids depicted at the 30% probability level (top). Atoms with a suffix ‘a’ are related through the 2-fold axis at the Ni atom. View of the metal core and the  $N4$  geometry about the Ni atom (middle). View of **4b** along the  $N2-Ni1$  axis and showing the  $H5/H32 \cdots Ni$  contacts with bond length and angle data included for this **4b** structure (bottom).

bond lengths are 1.879(2) Å and almost 0.1 Å shorter than in **4b** (though the 1.879(2) Å is regarded as unusually short for complexes of this type and due to the reduced ionic radius of

the  $d^8$  low spin and reduced inter-ligand steric interactions).<sup>6c</sup> In **4b**, these inter-ligand steric interactions are considerably increased due to the four flanking phenyl groups at C7 and C26 (and their symmetry equivalents) and resulting H5/H32...M contacts. In a Cambridge Structural Database study of Ni tetraza macrocycles, Donnelly and Zimmer have examined 150 such structures and correlated Ni–N distances revealing two distinct sets of low-spin (Ni–N < 2.02 Å) and high-spin (Ni–N > 2.05 Å) bond lengths.<sup>7</sup>

In complexes **4a–d**, differences of up to 7° are evident in some of the N–M–N bond angles (Table 1). For example, the N1–M–N1<sup>s</sup> angles are 131.25(16)° (Co), 134.3(2)° (Ni), 135.41(13)° (Cu) and 129.76(12)° (Zn) and with the analogous N3–M–N3<sup>s</sup> angles listed in Table 3 for comparisons (where symmetry operator  $S = 1/2 - x, 1/2 - y, z$ ). The interactions in **4a–d** comprise two intramolecular aromatic C–H...N hydrogen bonds, with two longer and weaker C–H... $\pi$ (arene) intermolecular interactions of note (Table 2). These four interactions are invariant across the four metal complexes. There are also several  $\pi$ ... $\pi$  stacking interactions with perpendicular ring to ring distances of *ca.* 3.5 Å to complete the myriad of weaker intermolecular interactions.

### <sup>1</sup>H NMR spectra

The paramagnetic copper complex **4c** gave, as might be expected, no recordable <sup>1</sup>H NMR spectra whereas the diamagnetic Zn complex **4d** gave a well resolved spectrum in the typical 0–10 ppm spectral region. Of more interest was the <sup>1</sup>H NMR of the Ni and Co complexes **4a** and **4b**, which displayed considerable positive

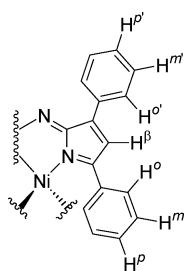
and negative peaks shifts (see ESI for Co spectra†).<sup>8</sup> Specifically, the spectrum of the Ni complex **4b** was recorded between –1.2 to 61.6 ppm at room temperature (Fig. 4). In the Ni<sup>II</sup> derivative, the electronic magnetic field is less effective at shortening the nuclear longitudinal relaxation times ( $T_1$ ) of the observed nuclei usually associated with paramagnetic complexes. Four-coordinate Ni<sup>II</sup> complexes preferably adopt a planar geometry, but with **2a** as the ligand this is sterically impossible and a pseudo-tetrahedral geometry results (Table 1 and Fig. 3). Nickel complexes of this geometry, which have short electron-spin lifetimes can allow well-resolved NMR signals to be obtained. Chemical shifts and integrated intensities observed for **4b** were as follows; –1.2 ppm (2H), 0.4 ppm (1H), 7.2 ppm (1H), 7.4 ppm (2H), 8.6 ppm (2H), 34.6 ppm (2H), and 61.7 ppm (1H) (Fig. 4). The  $D_2$  symmetry of **4b** makes the two ligands equivalent and provides a  $C_2$ -axis through the bridging nitrogen atoms and the central metal. This is confirmed by the chemical equivalence of both ligands and of opposing phenyl rings within each ligand. Resonance assignments are proposed based upon chemical shift, correlation spectra and on the measured  $T_1$  values (Table 3). zqTOCSY experiments revealed a correlation between the protons at –1.2, 0.4, and 7.4 ppm indicating that they belong to the same spin system (ESI†). These signals had measured  $T_1$  values of 64.5, 300 and 565 ms and are assigned to H<sup>o'</sup>, H<sup>m'</sup> and H<sup>p'</sup>, respectively, on the phenyl ring furthest from the metal centre (Table 3). The protons for the phenyl ring closer to the metal centre are assigned as the signals at 34.6, 8.6 and 7.2 ppm with measured  $T_1$  values of 2.2, 31.8 and 97.8 ms, respectively. A cross peak between the resonances at

**Table 2** H-bond interactions (bond lengths, Å; bond angles, °) in the metal complexes **4a–d**

	Metal, (M)	C15–H15...N2	C20–H20...N2	C12–H12...Cg1 <sup>a</sup>	C31–H31...Cg2 <sup>b</sup>
<b>4a</b>	Co	3.043(4)/116	3.029(4)/126	3.548(3)/137	3.606(3)/141
<b>4b</b>	Ni	3.053(5)/116	3.026(5)/126	3.548(6)/136	3.577(6)/142
<b>4c</b>	Cu	3.058(3)/115	3.029(3)/126	3.560(3)/138	3.602(3)/143
<b>4d</b>	Zn	3.043(3)/116	3.037(3)/126	3.547(3)/136	3.604(3)/141

<sup>a</sup> Cg1 is the five-membered ring centroid of {C17, C18, C25, C26, N3} at symmetry site  $-x, 1/2 - y, 1/2 + z$ . <sup>b</sup> Cg2 is the ring centroid of phenyl ring {C10...C15} at symmetry position  $1/2 + x, y, -1/2 + z$ .

**Table 3** <sup>1</sup>H NMR data for **4b**<sup>a</sup>

					
Resonance	$\delta$ /ppm	$T_1$ /ms	Resonance	$\delta$ /ppm	$T_1$ /ms
H <sup>o</sup>	34.6	2.2	H <sup>o'</sup>	–1.2	64.5
H <sup>m</sup>	8.6	31.8	H <sup>m'</sup>	7.4	300
H <sup>p</sup>	7.2	97.8	H <sup>p'</sup>	0.4	565
H <sup>β</sup>	61.6	21.2			

<sup>a</sup> Room temperature.

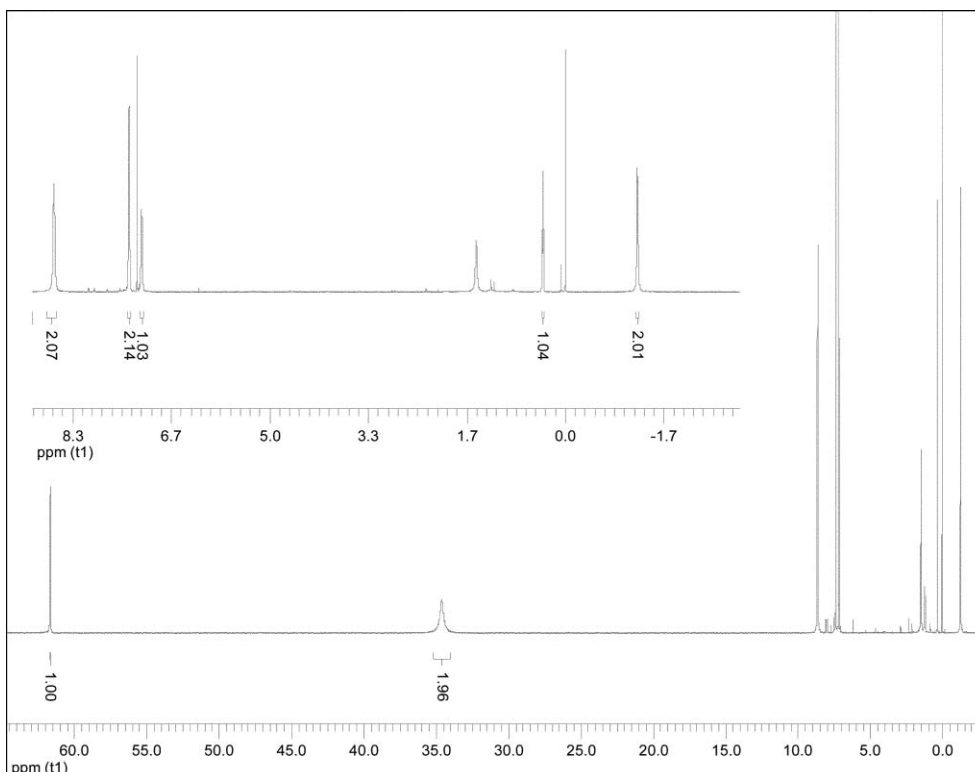


Fig. 4 600 MHz  $^1\text{H}$  NMR of **4b**. Inset shows an expansion between  $-2$  to  $9$  ppm.

8.6 and 7.2 ppm was observed in the zqTOCSY but not for the 34.6 ppm resonance potentially due to the broad nature of this signal,  $\Delta\nu_{1/2} > 170$  Hz, (ESI $^\dagger$ ). Despite this, the signal at 34.6 ppm does show a relative integral for 2H, implying it must be either the *ortho* or *meta* protons. The  $T_1$  value of 2.2 ms for this signal was the shortest of any resonance in **4b** and an examination of the crystal structure shows that the *ortho* protons ( $\text{H}^o$ ) are the closest to the metal (2.67/2.78 Å) and as such would be expected to have the shortest  $T_1$  (Fig. 3 bottom and Table 1).<sup>9</sup> Accordingly, the 8.6 and 7.2 ppm resonances are assigned as  $\text{H}^m$  and  $\text{H}^o$ , respectively. The signal at 61.6 ppm ( $T_1 = 21.2$  ms) is assigned to the  $\beta$ -proton on the pyrrole ring.

### Absorbance spectra

The UV-vis spectra for the complexes **4a**, **4b** and **4d** display similar spectral characteristics with the  $\lambda_{\text{max}}$  values between 593–603 nm in  $\text{CH}_2\text{Cl}_2$  and extinction coefficients varying from 65 000–142 000  $\text{M}^{-1}\text{cm}^{-1}$  (Table 4). Uniquely, the copper complex **4c** showed a clear splitting of the longest wavelength band with  $\lambda$  values of 566–640 nm, which may be indicative of the strain within the ligand while the other complexes exhibited distinct red-shifted shoulders of the main absorption band. Minor hypsochromic shifts in ethanol and bathochromic shifts in toluene were observed in each case. The similarity of the metal chelates with the free ligand **2a** ( $\lambda_{\text{max}}$  593 nm in  $\text{CH}_2\text{Cl}_2$ ) suggests the absorption is primarily ligand centred with band broadening and minor hypsochromic shifts observed upon metal chelation. In contrast to the  $\text{BF}_2$  chelated derivatives **1**, each of the complexes **4a–d** were non-fluorescent.

### EPR spectra

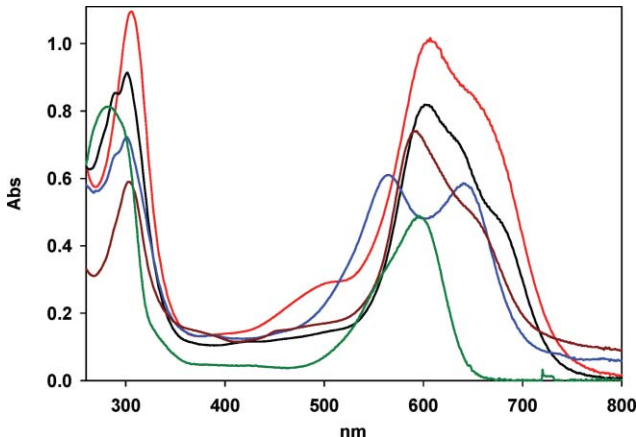
In  $D_2$  symmetry, the degeneracy of all five d orbitals is, in principle, lifted. However, if we consider the geometry as a distortion from “tetrahedral” (actually  $D_{2d}$ ) via twisting of the two ligand planes, then we might reasonably expect a  $(z^2)(x^2 - y^2)(xz, yz)(xy)$  ordering, where  $z$  is the bisector of the normals to the ligand planes. On this basis, the  $\text{Co}^{\text{II}}$   $d^7$  compound **4a** has  $S = 3/2$  [ $(z^2)^2(x^2 - y^2)^2(xz, yz)^2(xy)^1$ ] and EPR spectra should be observable because of its orbital singlet nature.

Indeed, as the temperature is decreased below *ca.* 40 K, intense EPR transitions grow in at 0.94, 6.6 and 8.0 kG at X-band (Fig. 5; at lower temperatures a further feature grows in at 3.3 kG, we are unsure of its origin). These can be read as effective  $g$  values ( $g^{\text{eff}} = 7.4, 1.1$  and  $0.87$ ) due to transitions within the ground Kramers doublet ( $M_S = \pm 1/2$  or  $\pm 3/2$ ), which must be well separated from the upper doublet by  $2D \gg h\nu$ , where  $D$  is the axial zero-field splitting (ZFS) parameter defined in spin Hamiltonian (eqn (1)).<sup>10</sup> This situation is common for pseudo-tetrahedral  $\text{Co}^{\text{II}}$  species, and similar spectra have been observed for [ $\{\text{H}_2\text{B}(\text{pz})_2\}_2\text{Co}$ ] ( $\text{H}_2\text{B}(\text{pz})_2$  = dihydrobis(1-pyrazolyl)borate), which also has a  $\text{CoN}_4$  coordination sphere.<sup>11</sup>

$$H = \mu_B B g \hat{S} + D[\hat{S}_z^2 - S(S+1)/3] + E(\hat{S}_x^2 - \hat{S}_y^2) \quad (1)$$

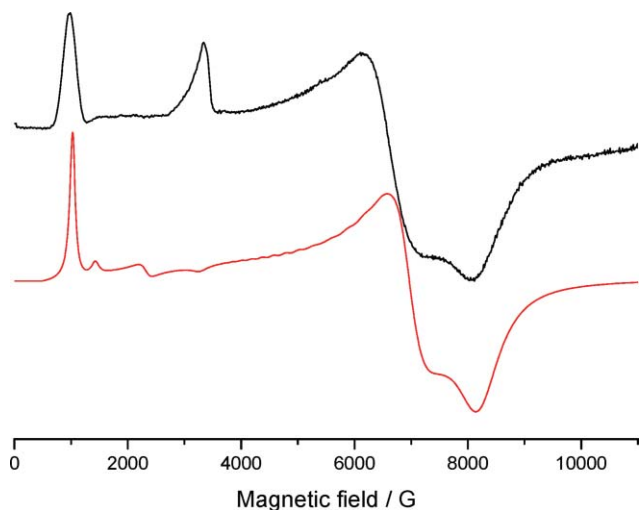
The assignment is confirmed by W-band (94 GHz) spectra at 10 K, where now only one transition is observed, with  $g^{\text{eff}} = 7.2$ , the low  $g^{\text{eff}}$  features being beyond the 6 T limit of the magnet. Pilbrow has considered the  $g^{\text{eff}}$  values that arise for large positive and negative  $D$  as a function of the rhombic ZFS parameter  $E$  (eqn (1)).<sup>10</sup> It is clear from his results that  $g^{\text{eff}} < 1$  can only easily arise within the  $M_S = \pm 3/2$  doublet: assuming  $g = 2.0$ , values



**Table 4** Comparative UV-vis spectra of **2a** and **4a–d**<sup>a, b</sup>


Compound	CH <sub>2</sub> Cl <sub>2</sub> $\lambda_{\text{max}}$ /nm	EtOH $\lambda_{\text{max}}$ /nm	Toluene $\lambda_{\text{max}}$ /nm	$\epsilon/\text{M}^{-1}\text{cm}^{-1}$ <sup>c, d</sup>
<b>2a</b> (green)	596	592	601	52.4
<b>4a</b> (black)	602	599	607	94
<b>4b</b> (red)	603	599	606	142
<b>4c</b> (blue)	640/567	639/562	642/567	65.7/62.8
<b>4d</b> (brown)	593	590	596	78.6

<sup>a</sup> Shown in CH<sub>2</sub>Cl<sub>2</sub>. <sup>b</sup> (8.7–9.1 × 10<sup>−6</sup> M). <sup>c</sup> CH<sub>2</sub>Cl<sub>2</sub>. <sup>d</sup> × 10<sup>−3</sup>.

**Fig. 5** X-band EPR spectrum of a powder of **4a** at 10 K (black) and simulation (red) with the parameters:  $S = 3/2$ ,  $g_z = 2.3$ ,  $g_{x,y} = 2.0$ ,  $E/D = -0.16$  where  $D$  is negative and  $|D| > \text{ca. } 15 \text{ cm}^{-1}$ .

of  $g_{z,x,y}^{\text{eff}} = 6, 0, 0$  or  $5.464, 2.0, 1.464$  are derived for the limiting cases of  $|E/D| = 0$  (axial symmetry) and  $1/3$  (rhombic limit), respectively, ( $E/D > 1/3$  implies a redefinition of axes). Although non-coincidence between the principal axes of the  $g$  matrix and  $D$  tensor can give rise to unusual  $g^{\text{eff}}$  within  $M_S = \pm 1/2$ ,<sup>12</sup> this is not allowed in the  $D_2$  symmetric **4a**. Hence, the ground state doublet in **4a** is  $M_S = \pm 3/2$  (*i.e.*  $D$  is negative). We can simulate the spectra (X- and W-band) using spin Hamiltonian (eqn (1)) with  $S = 3/2$ . As the limiting values above suggest,  $g_z^{\text{eff}}$  and  $g_{x,y}^{\text{eff}}$  are very sensitive to the ratio  $E/D$ . We initially fixed an isotropic  $g = 2.0$  and varied  $E/D$  for an arbitrarily large, negative value of  $D$ . The best fit to the

$g_z^{\text{eff}} = 1.1$  and  $0.87$  resonances is found for  $|E/D| = 0.16$  (Fig. 5); further refinement to fit  $g_z^{\text{eff}}$  gives  $g_z = 2.3$ . Although this procedure does not define the magnitude of  $|D|$ , from systematic variations it must be greater than *ca.*  $15 \text{ cm}^{-1}$ , since for values below this we should observe transitions within the excited  $M_S = \pm 1/2$  doublet (the  $3.3 \text{ kG}$  feature is not consistent with such transitions). Note the ZFS is much more sensitive than the  $g$  values to deviations of the symmetry from axial.

The Ni<sup>II</sup>  $d^8$  complex **4b** is EPR silent at all frequencies (X- and W-band) and temperatures (300–4.2 K) studied, despite its paramagnetism. Adopting the same  $d$  orbital ordering we have  $(z^2)^2(x^2 - y^2)^2(xz, yz)^3(xy)^1$ , hence the ground term is a spin triplet but an orbital doublet. The orbital moment gives rise to rapid electronic relaxation, which can broaden EPR spectra beyond detection. A further consequence is that relatively sharp NMR spectra are observed, see above, in contrast with the orbital singlet Co<sup>II</sup> species.

Powder EPR spectra of the Cu<sup>II</sup>,  $d^9$  complex **4c** appear axial at X-band but are in fact slightly rhombic as resolved at K-band (24 GHz) frequency ( $g = 2.25, 2.08, 2.06$ , Fig. 6). In frozen solution, the spectra are axial within the resolution of K-band, implying that the structure relaxes slightly in solution, consistent with the NMR spectra of the nickel analogue (see above). The X-band frozen solution spectra show hyperfine coupling to both <sup>63,65</sup>Cu and to <sup>14</sup>N nuclei, which can be simulated with the ( $S = 1/2$ ) spin-Hamiltonian parameters:  $g_z = 2.248$ ,  $g_{x,y} = 2.065$ ,  $A_z(\text{Cu}) = 115 \text{ G}$ ,  $A_{x,y}(\text{Cu}) = 16 \text{ G}$ ,  $A_{x,y}(4 \times \text{N}) = 9.0 \text{ G}$  and an arbitrarily small  $A_z(\text{N})$  (see, ESI†).

Note the near-axial  $g$  values imply the  $xz, yz$  pair are near-degenerate  $[(z^2)^2(x^2 - y^2)^2(xz, yz)^4(xy)^1]$  although this is not imposed in  $D_2$  (indeed in the solid state we observe  $g_x \neq g_y$ ).  $D_2$  does require that the principal axes of the  $g$  and  $A(\text{Cu})$  matrices are coincident and that they are co-parallel with the three two-fold

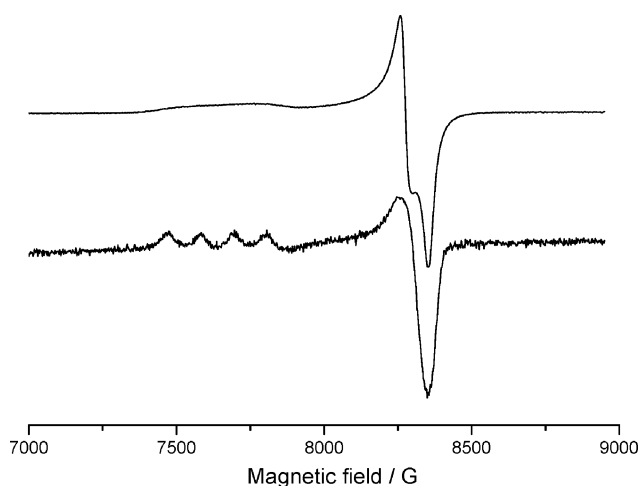


**Fig. 6** K-band (ca. 24 GHz) EPR spectra of a powder (top) and a frozen  $\text{CH}_2\text{Cl}_2$ -toluene (10 : 1 v/v) solution (bottom) of **4c**.

symmetry axes of the molecule. Since we expect the largest  $g$  and  $A$  to be normal to the  $xy$  magnetic orbital we assign these as  $z$ . This assignment is also consistent with the observation of the large component of the (four equivalent)  $^{14}\text{N}$  hyperfine in the  $xy$  plane (see, ESI†).

## Conclusion

The synthesis, solution and solid state spectral properties of four divalent metal complexes of the tetraphenylazadipyrromethene ligand are described, which should facilitate future designed studies and applications.

## Experimental

### General

Compound **2a** was synthesised as described in ref. 1b. The complexes' formation reactions were carried out exposed to air.

#### Bis[(3,5-diphenyl-1H-pyrrol-2-yl)(3,5-diphenylpyrrol-2-ylidene)amine]Co<sup>II</sup> (**4a**)

Compound **2a** (0.20 g, 0.445 mmol) and ammonium acetate (0.20 g, 2.6 mmol) in *n*-butanol (7 mL) were added to a solution of cobalt<sup>II</sup> chloride hexahydrate (0.130 g, 0.548 mmol) in *n*-butanol (3 mL). The mixture was stirred for 1 h at reflux, cooled to room temperature and the precipitate filtered as a dark brown powder (0.15 g, 70%), mp: >300 °C (decomposition).  $^1\text{H}$  NMR ( $\text{CDCl}_3$ , 600 MHz)  $\delta$ /ppm: 64.38 (m, 4H), 16.14 (m, 8H), 14.40 (m, 8H), 8.98 (m, 8H), 6.20 (m, 4H), 4.60 (m, 4H), -13.52 (m, 8H). UV-vis ( $\text{CH}_2\text{Cl}_2$ )  $\lambda_{\text{max}}$ /nm: 602. ES-MS ( $m/z$ ):  $[\text{M} + \text{H}]^+$  956.2. HRMS: calcd for  $\text{C}_{64}\text{H}_{45}\text{N}_6\text{Co}$ :  $[\text{M} + \text{H}]^+$  956.3038, found: 956.3063. IR (KBr disc)  $\nu/\text{cm}^{-1}$ : 1519, 2920. Crystals were grown by the slow evaporation of a chlorobenzene solution.

#### Bis[(3,5-diphenyl-1H-pyrrol-2-yl)(3,5-diphenylpyrrol-2-ylidene)amine]Ni<sup>II</sup> (**4b**)

Compound **2a** (0.30 g, 0.668 mmol) and nickel<sup>II</sup> acetate (0.160 g, 0.904 mmol) in *n*-butanol (15 mL) was stirred for 1 h at reflux,

cooled to room temperature and the precipitate filtered as a red/brown powder (0.261 g, 82%), mp: 326–327 °C.  $^1\text{H}$  NMR ( $\text{CDCl}_3$ , 600 MHz)  $\delta$ /ppm: -1.22 (d, 8H,  $J = 7.38$  Hz), 0.38 (t, 4H,  $J = 6.90$  Hz), 7.17 (bs, 4H), 7.38 (t, 8H,  $J = 7.02$  Hz), 8.65 (bs, 8H), 34.62 (bs, 8H), 61.67 (s, 4H).  $^{13}\text{C}$  NMR ( $\text{CDCl}_3$ , 151 MHz)  $\delta$ /ppm: 21.5, 85.1, 107.2, 126.4, 129.1, 155.6, 159.3, 193.6, 201.3, 225.2, 499.3, 500.4, 751.0. UV-vis ( $\text{CH}_2\text{Cl}_2$ )  $\lambda_{\text{max}}$ /nm: 603. ES-MS ( $m/z$ ):  $[\text{M} + \text{H}]^+$  955.2. HRMS: calcd for  $\text{C}_{64}\text{H}_{45}\text{N}_6\text{Ni}$ :  $[\text{M} + \text{H}]^+$  955.3059, found: 955.3087. IR (KBr disc)  $\nu/\text{cm}^{-1}$ : 1260, 1447, 1519, 2922. Crystals were grown by the slow evaporation of a DMF solution.

#### Bis[(3,5-diphenyl-1H-pyrrol-2-yl)(3,5-diphenylpyrrol-2-ylidene)amine]Cu<sup>II</sup> (**4c**)

Compound **2a** (0.30 g, 0.668 mmol) and copper<sup>II</sup> acetate (0.150 g, 0.8228 mmol) in *n*-butanol (15 mL) was stirred for 1 h at reflux, cooled to room temperature and the precipitate filtered as a black powder, (0.240 g, 75%), mp: >300 °C (decomposition). UV-vis ( $\text{CH}_2\text{Cl}_2$ )  $\lambda_{\text{max}}$ /nm: 566, 640. ES-MS ( $m/z$ ):  $[\text{M} + \text{H}]^+$  960.3. HRMS calcd for  $\text{C}_{64}\text{H}_{45}\text{N}_6\text{Cu}$ :  $[\text{M} + \text{H}]^+$  960.3002, found: 960.3033. IR (KBr disc)  $\nu/\text{cm}^{-1}$ : 1365, 1447, 1519, 2918. Crystals were grown by the slow evaporation of a DMF solution.

#### Bis[(3,5-diphenyl-1H-pyrrol-2-yl)(3,5-diphenylpyrrol-2-ylidene)amine]Zn<sup>II</sup> (**4d**)

Compound **2a** (0.30 g, 0.668 mmol) and zinc<sup>II</sup> acetate (0.1586 g, 0.869 mmol) in *n*-butanol (15 mL) was stirred for 1 h at reflux, cooled to room temperature and the precipitate filtered as a dark green powder (0.273 g, 85%), mp: 312–313 °C.  $^1\text{H}$  NMR (400 MHz,  $\text{CDCl}_3$ )  $\delta$ /ppm: 6.71 (s, 4H), 7.09 (m, 12H), 7.40 (m, 12H), 7.49 (m, 8H) 7.85 (m, 8H).  $^{13}\text{C}$  NMR ( $\text{CDCl}_3$ , 101 MHz)  $\delta$ /ppm: 117.05, 126.82, 127.55, 127.99, 128.04, 129.12, 129.70, 133.24, 134.35, 145.25, 147.88, 160.43. UV-vis ( $\text{CH}_2\text{Cl}_2$ )  $\lambda_{\text{max}}$ /nm: 593. ES-MS ( $m/z$ ):  $[\text{M} + \text{H}]^+$  961.6. HRMS calcd for  $\text{C}_{64}\text{H}_{45}\text{N}_6\text{Zn}$ :  $[\text{M} + \text{H}]^+$  961.3022, found: 961.2997. IR (KBr disc)  $\nu/\text{cm}^{-1}$ : 1246, 1542, 2922. Crystals were grown by the slow evaporation of a DMF solution.

### X-Ray data collection, structure solution and refinement

Data were collected on a Bruker SMART APEX CCD diffractometer for **1a** at room temperature (293 K) and for **4a–d** at 100 K. Data were collected on a hemisphere of reciprocal space using  $\phi$ - $\omega$  scans with an empirical absorption correction applied using SADABS.<sup>13</sup> All four Co, Ni, Cu and Zn metal complexes **4a–d** are isomorphous structures in the space group (*Fdd2*, no. 43). Solution and refinement was undertaken using SHELXS-97 and SHELXL-97<sup>14</sup> and the graphics generated with PLATON.<sup>15</sup> Hydrogen atoms were included as riding atoms in **4a–d** with the SHELXL-97 defaults at the appropriate temperatures. Pertinent geometric data for structures **4a–d** are included in Table 1–3.

Crystallographic data for **4b** (representative of **4a–d**). **4b**, chemical formula  $\text{C}_{64}\text{H}_{44}\text{N}_6\text{Ni}$ , black blocks, molecular weight = 955.76 g mol<sup>-1</sup>, orthorhombic, space group *Fdd2* (no. 43),  $a = 19.842(3)$ ,  $b = 44.333(5)$ ,  $c = 10.7588(14)$  Å,  $V = 9464(2)$  Å<sup>3</sup>,  $Z = 8$ ,  $T = 100(2)$  K,  $D_{\text{calcd}} = 1.342$  g cm<sup>-3</sup>,  $F(000) = 3984$ ,  $\mu = 0.461$  mm<sup>-1</sup>, 9708 reflections to  $\theta = 24.2^\circ$ , 3176 unique (with 2642  $I > 2\sigma(I)$ ), 322 parameters,  $R$  factor is 0.047,  $wR_2 = 0.087$ .

(based on  $F^2$  for with  $I > 2\sigma(I)$ ) using SHELXL-97 as the refinement program, GOF = 1.03, density range in final  $\Delta$  map is  $-0.58$  to  $+0.40$  e  $\text{\AA}^{-3}$ .

## Acknowledgements

AO and DOS acknowledge funding support from the Program for Research in Third-Level Institutions administered by the HEA. Thanks to Dr D. Rai of the CSCB Mass Spectrometry Centre and Dr J. Muldoon and Dr Y. Ortin of the CSCB NMR facility. JW and EJMI thank EPSRC (UK) for funding and Prof. D. Collison for helpful discussions.

## Notes and references

- (a) J. Killoran, L. Allen, J. F. Gallagher, W. M. Gallagher and D. F. O'Shea, *Chem. Commun.*, 2002, 1862; (b) A. Gorman, J. Killoran, C. O'Shea, T. Kenna, W. M. Gallagher and D. F. O'Shea, *J. Am. Chem. Soc.*, 2004, **126**, 10619; (c) S. O. McDonnell, M. J. Hall, L. T. Allen, A. Byrne, W. M. Gallagher and D. F. O'Shea, *J. Am. Chem. Soc.*, 2005, **127**, 16360; (d) W. M. Gallagher, L. T. Allen, C. O'Shea, T. Kenna, M. Hall, J. Killoran and D. F. O'Shea, *Br. J. Cancer*, 2005, **92**, 1702; (e) M. J. Hall, S. O. McDonnell, J. Killoran and D. F. O'Shea, *J. Org. Chem.*, 2005, **70**, 5571; (f) J. Killoran, J. F. Gallagher, P. V. Murphy and D. F. O'Shea, *New J. Chem.*, 2005, **29**, 1258; (g) J. Killoran and D. F. O'Shea, *Chem. Commun.*, 2006, 1503; (h) S. O. McDonnell and D. F. O'Shea, *Org. Lett.*, 2006, **8**, 3493; (i) M. J. Hall, L. T. Allen and D. F. O'Shea, *Org. Biomol. Chem.*, 2006, **4**, 776; (j) D. F. O'Shea, J. Killoran, and W. M. Gallagher, *US Pat.*, 7 220 732, 2007; (k) J. Killoran, S. O. McDonnell, J. F. Gallagher and D. F. O'Shea, *New J. Chem.*, 2008, **32**, 483; (l) A. Loudet, R. Bandichhor, K. Burgess, A. Palma, S. O. McDonnell, M. J. Hall and D. F. O'Shea, *Org. Lett.*, 2008, **10**, 4771.
- (a) R. E. Gawley, H. Mao, M. Mahbubul Haque, J. B. Thorne and J. S. Pharr, *J. Org. Chem.*, 2007, **72**, 2187; (b) A. Coskun, M. Deniz, Yilmaz and E. U. Akkaya, *Org. Lett.*, 2007, **9**, 607.
- M. A. T. Rogers, *J. Chem. Soc.*, 1943, 590.
- T. S. Teets, D. V. Partyka, A. J. Esswein, J. B. Updegraff III, M. Zeller, A. D. Hunter and T. G. Gray, *Inorg. Chem.*, 2007, **46**, 6218.
- During the completion of this manuscript, the  $\text{Zn}^{\text{II}}$  complex appeared in the literature: T. S. Teets, D. V. Partyka, J. B. Updegraff III and T. J. Gray, *Inorg. Chem.*, 2008, **47**, 2338.
- (a) For representative examples see: J. E. Fergusson and C. A. Ramsey, *J. Chem. Soc.*, 1965, 5222; (b) Y. Murakami, Y. Matsuda and K. Sakata, *Inorg. Chem.*, 1971, **10**, 1728; (c) C. Brückner, V. Karunaratne, S. J. Rettig and D. Dolphin, *Can. J. Chem.*, 1996, **74**, 2182; (d) S. R. Halper, M. R. Malachowski, H. M. Delaney and S. M. Cohen, *Inorg. Chem.*, 2004, **43**, 1242; (e) L. Do, S. R. Halper and S. M. Cohen, *Chem. Commun.*, 2004, 2662; (f) L. Yu, K. Muthukumaran, I. V. Sazanovich, C. Kirmaier, E. Hindin, J. R. Diers, P. D. Boyle, D. F. Bocian, D. Holten and J. S. Lindsey, *Inorg. Chem.*, 2003, **42**, 6629.
- M. A. Donnelly and M. Zimmer, *Inorg. Chem.*, 1999, **38**, 1650.
- (a) Examples of  $^1\text{H}$  NMR spectra of nickel<sup>II</sup> and cobalt<sup>II</sup> complexes see: E. Szajna, P. Dobrowolski, A. L. Fuller, A. M. Arif and L. M. Berreau, *Inorg. Chem.*, 2004, **43**, 3988; (b) A. Sánchez-Méndez, J. M. Benito, E. de Jesús, F. J. de la Mata, J. C. Flores, R. Gomez and P. Gómez-Sal, *Dalton Trans.*, 2006, 5379; (c) R. Knorr, H. Hauer, A. Weiss, H. Polzer, F. Ruf, P. Löw, P. Dvortsák and P. Böhrer, *Inorg. Chem.*, 2007, **46**, 8379; (d) E. C. Constable, R. Martínez-Mañez, A. M. W. Cargill-Thompson and J. V. Walker, *J. Chem. Soc., Dalton Trans.*, 1994, 1585; (e) H. Amouri, L. Mimassi, M. N. Rager, B. E. Mann, C. Guyard-Duhayon and L. Raehm, *Angew. Chem., Int. Ed.*, 2005, **44**, 4543; (f) R. L. Paul, Z. R. Bell, J. C. Jeffery, J. A. McCleverty and M. D. Ward, *Proc. Natl. Acad. Sci. U. S. A.*, 2002, **99**, 4883.
- Salomon, *Phys. Rev.*, 1955, **99**, 559.
- J. R. Pilbrow, *J. Magn. Reson.*, 1978, **31**, 479.
- L. J. Guggenberger, C. T. Prewitt, P. Meakin, S. Trofimenko and J. P. Jesson, *Inorg. Chem.*, 1973, **12**, 508.
- Bencini and D. Gatteschi, *Inorg. Chem.*, 1977, **16**, 2141.
- G. M. Sheldrick, *SADABS, Program for area detector adsorption correction*, Institute for Inorganic Chemistry, University of Göttingen, Germany, 1996.
- (a) G. M. Sheldrick, *Acta Crystallogr., Sect. A: Found. Crystallogr.*, 2008, **64**, 112; (b) P. McArdle, *J. Appl. Crystallogr.*, 1995, **28**, 65.
- A. L. Spek, *J. Appl. Crystallogr.*, 2003, **36**, 7.